

REPLACEMENT COPY  
SUBJECT TO RECALL  
IN TWO WEEKS

Aluminum-Air Power Cell Research and Development  
Annual Report Summary, CY1984

A. Maimoni

February 27, 1985

Lawrence  
Livermore  
National  
Laboratory

This is an informal report intended primarily for internal or limited external distribution. The opinions and conclusions stated are those of the author and may or may not be those of the Laboratory.

Work performed under the auspices of the U.S. Department of Energy by the Lawrence Livermore National Laboratory under Contract W-7405-Eng-48.

## DISCLAIMER

This document was prepared as an account of work sponsored by an agency of the United States Government. Neither the United States Government nor the University of California nor any of their employees, makes any warranty, express or implied, or assumes any legal liability or responsibility for the accuracy, completeness, or usefulness of any information, apparatus, product, or process disclosed, or represents that its use would not infringe privately owned rights. Reference herein to any specific commercial product, process, or service by trade name, trademark, manufacturer, or otherwise, does not necessarily constitute or imply its endorsement, recommendation, or favoring by the United States Government or the University of California. The views and opinions of authors expressed herein do not necessarily state or reflect those of the United States Government or the University of California, and shall not be used for advertising or product endorsement purposes.

This report has been reproduced  
directly from the best available copy.

Available to DOE and DOE contractors from the  
Office of Scientific and Technical Information  
P.O. Box 62, Oak Ridge, TN 37831  
Prices available from (615) 576-8401, FTS 626-8401

Available to the public from the  
National Technical Information Service  
U.S. Department of Commerce  
5285 Port Royal Rd.,  
Springfield, VA 22161

## INTRODUCTION

The objective of the Aluminum-Air Power Cell program is to develop an automotive energy source for general purpose vehicles, and evaluate its ability to provide vehicles with the range, acceleration performance, and rapid refueling capability of current internal combustion engine vehicles. The main components of the system are shown in Fig. 1.

The Lawrence Livermore National Laboratory (LLNL) provides program direction. Most of the work is done under a main cost shared contract with Eltech Systems Corp. Eltech has formed a consortium with Alcan Aluminum Ltd., Case Western Reserve University (CWRU), and SRI International. The main thrust of research during 1984 was: a) air cathode development, b) hydrargillite crystallization and separation, c) integrated experiments involving a coupled cell/crystallizer, d) cell design, and e) development of improved aluminum anodes.

The development work has treated anode development, cell design, and crystallization development as independent problems. The close coupling between these aspects of the problem can no longer be ignored and will receive increased emphasis during 1985.

## SYSTEMS ANALYSIS

LLNL provided inputs to JPL's study for OVERD and to Aerospace Corp. for their Hardware Performance Status - 1984 report.<sup>1</sup> The information will be revised in FY1986, when the initial complete design of a vehicular aluminum-air system is performed. The energy efficiency of the aluminum-air system is discussed below.

### Energy Efficiency

The comparison of aluminum-air power cell to internal combustion engine (ICE) and to rechargeable battery vehicles was performed on the basis of energy delivered to the vehicle power train, i.e., the transmission input shaft, using coal as a common energy source.

Internal combustion engine: One of the best technologies for manufacturing synthetic high octane gasoline from coal is the Mobil zeolite

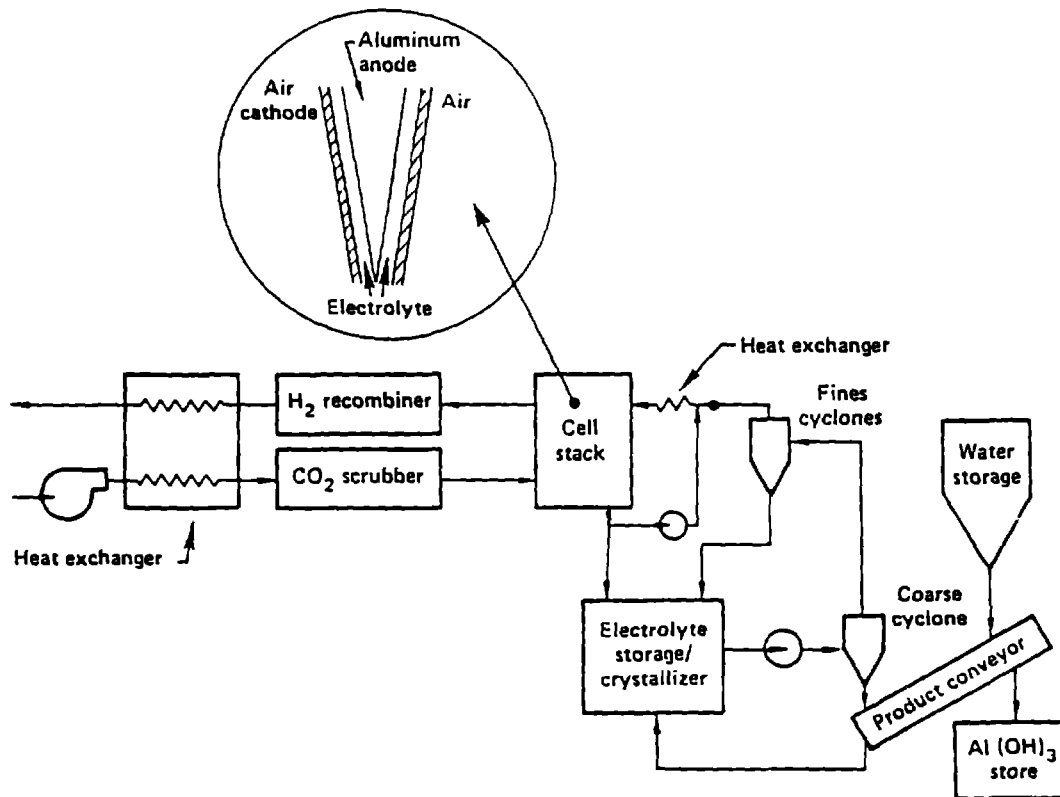


Fig. 1. Aluminum-Air Power Cell schematic flow diagram. There are three independent circulation flows: (1) the incoming air which enters the cell stack after CO<sub>2</sub> removal, preheating, and humidifying, (2) the cell-stack-electrolyte circulation loop which goes through a heat exchanger to remove excess heat from the system, and (3) the cell-crystallizer exchange flow which goes through particle-size separation devices for final hydrargillite product removal and removal of most of the particles from the electrolyte before return to the cell.

process; its overall energy efficiency is about 50%. The efficiency of an ICE is about 18% over the SAE J227a(D) test cycle.<sup>2</sup> Combining the above efficiencies, the overall efficiency of an ICE based on coal derived fuels is about 9%.

Electric Vehicles: The efficiency of advanced coal-based power plants is about 39% and the efficiency of a motor-controller for an EV is about 85%.

- a) Rechargeable EV: If the charge/discharge cycle has an efficiency of 70%, the overall efficiency of the rechargeable EV is  $.7 \times .85 \times .39$  or about 23%.
- b) Aluminum-air EV: The efficiency of aluminum production is

usually given in kWh/kg of aluminum. It is 11.3 kWh/kg for the best commercially reported Hall process, and 8.3 kWh/kg for the Alcoa Smelting process. Presently available materials yield about 4.5 kWh/Kg of aluminum in the aluminum-air cell.<sup>3</sup> Our goal is 6.5 kWh/Kg. From these values one obtains the range of energy efficiencies of the aluminum-air system:

Hall process,<sup>3</sup> currently available materials for Al-air cell:  
 $39\% \times 85\% \times 4.7/11.3 = 14\%$

Alcoa Smelting,<sup>3</sup> currently available materials for Al-air cell:  $39\% \times 85\% \times 4.7/8.3 = 18\%$

Alcoa Smelting, anticipated improvements in Al-air materials performance:  $39\% \times 85\% \times 6.5/8.3 = 25\%$  .

## INTEGRATED EXPERIMENTS

Two experiments were performed at LLNL during 1984 in which a single cell was coupled to a crystallizer to simulate the performance of an aluminum-air power cell system. Both experiments ran for about 5 h at 120 A nominal current. While both experiments suffered from failures in the tubing of the peristaltic pump tubing feeding the hydrocyclone, which precluded obtaining good material balances and relating crystal growth parameters to operational conditions, a great deal of important system design information was obtained.

### M3-3 Experiment

A report describing the M3-3 experiment in detail will be published in March 1985.<sup>4</sup> In the M3-3 experiment, Fig. 2, the M3 cell was run at 14 A for 101 min, followed by 122 A for 269 min at 60°C with 4M NaOH electrolyte containing 0.06M sodium stannate as corrosion inhibitor; the overall current efficiency was 96%. Previous experiments used a commercial hydrocyclone sized for 30 to 50 cells; the M3-3 experiment used a hydrocyclone scaled for 1 to 5 cells. Peristaltic pumps were used instead of the centrifugal pumps from previous experiments; essentially no particle degradation occurred when peristaltic pumps were used to feed a hydrocyclone.<sup>5</sup>

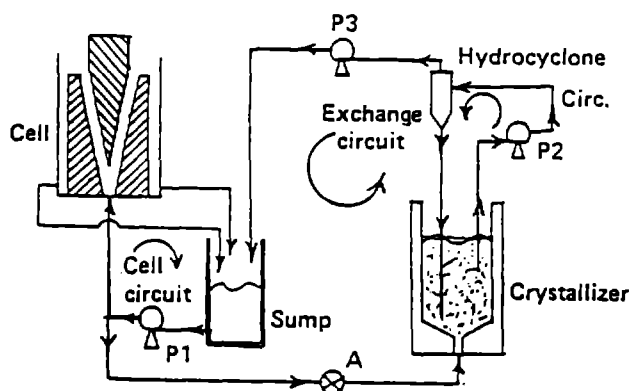


Fig. 2. Flow diagram for M3-3 experiment. There are two independent circulation loops: (1) cell recirculation loop, and (2) exchange flow between cell and the crystallizer. Exchange flow is regulated by pump P3 and valve A.

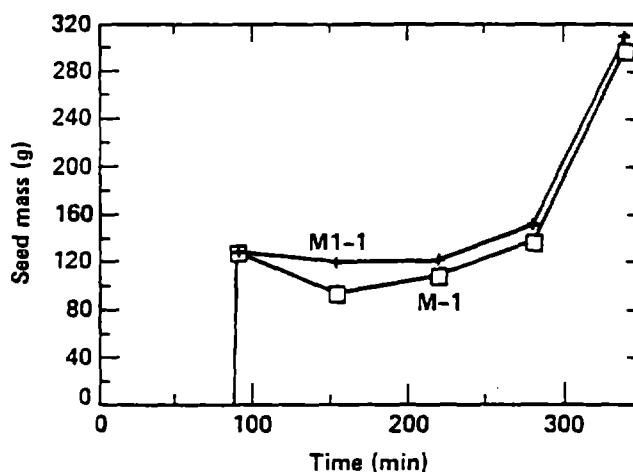


Fig. 3. Comparison of seed mass calculated from material balance (M-1) with that calculated by integration of Alcoa's rate equation (M1-1). The initial drop in the value of M-1 is due to dissolution.

Analysis of the results obtained in the M3-3 experiment indicates reasonable agreement in the material balances, and in a comparison between the calculated M1-1 and experimental M-1 values of the mass of hydrargillite in the system, Fig. 3.

A more sensitive test of the material balances is the evolution in total crystal population as a function of time, given as the base 10 logarithm of the particle population for various times in Fig. 4. The main conclusion derived from Fig. 4 is that at 60°C secondary nucleation produced an approximately 100-fold increase in the total number of fine particles. The

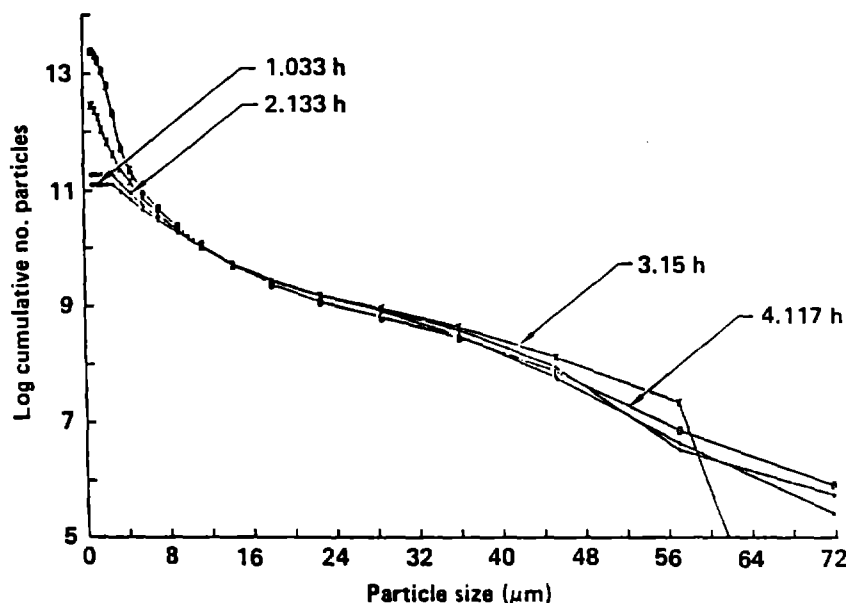


Fig. 4. Total particle population in the system at various times shown as the logarithm (base 10) of the total number of particles. The population of fine particles increased over 100 fold throughout the course of the experiment.

time averaged value of particle growth rate for particles larger than about 17  $\mu\text{m}$  was approximately size independent, at about 1.2  $\mu\text{m}/\text{h}$ .

#### M4-1 Experiment

The M4-1 experiment was the initial test of the M4 "reference cell", shown in Fig. 5. It was also the initial test of a new crystallizer and interconnecting piping; the first operation of coupled cell-crystallizer system at temperatures in the 70-80°C range; the initial test of a new data acquisition system; the initial operational test of on-line Foxboro conductivity meters; and, the initial use at LLNL of a modified industry standard method for the determination of sodium and aluminate concentrations.

Most of the new components performed very well. The main operational problems were failures of the peristaltic pump tubing, accumulation of gas in one of the Foxboro meter housings, and plugging of electrolyte return line from the cell by metallic tin and hydrargillite. The precipitation rate of tin in the 70-80°C range was approximately linear with time, about 17% of the initial tin content per hour. The M4-1 experiment was terminated when the electrolyte return from the cell began to overflow, due to plugging of the

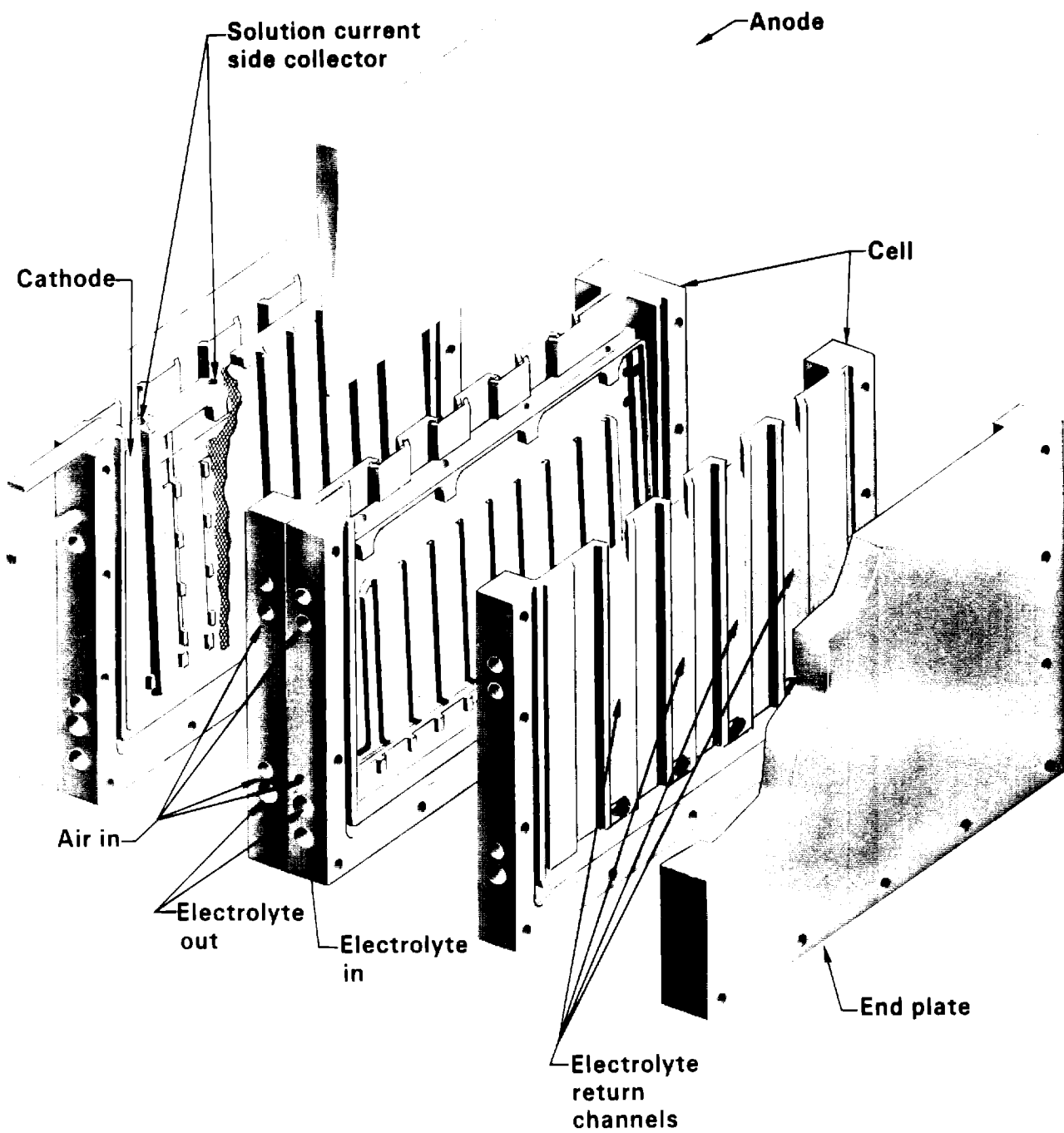


Fig. 5. The M4 Aluminum-Air Wedge Cell.

return flow to the crystallizer. The flow restriction that led to overflow in the cell return is likely to have occurred in the return line to the crystallizer.

The conditions required to obtain representative samples of the solids were determined prior to the M4-1 test; particle size distribution data are still being analyzed. Detailed information about performance of the various system components is given in the following sections.

## INDIVIDUAL COMPONENTS

### Air Cathode

Work in this important area has continued at Eltech, Electromedia, and Case Western Reserve University (CWRU). In previous work<sup>6</sup> the best electrode to date had a life in excess of 1400 cycles, equivalent to over two years operating life in a vehicle. While attempts to duplicate this performance have not been as yet successful, a great deal has been learned about the effect on operating life of various materials and fabrication variables. A number of steam activated carbon blacks have performance as good as that of activated carbons; the most promising materials are classified RBDA and Norit Ultracarbon, containing a 5-10% loading of CoTMPP. Electromedia has obtained substantial improvement in the polarization characteristics of the air electrodes as well as significant improvements in electrode life by using an alternative binder material instead of Teflon and increasing the thickness of the wet-proof and active layers.

Work at CWRU has concentrated on three main areas:

- 1) Understanding the role of the transition metal. A transition metal is required, but it can be incorporated before or after heat treatment. Almost the same degree of activity was obtained when carbons with adsorbed H<sub>2</sub>TMPP were treated with solutions of the transition metal. After heat treatment to 450°C and 800°C some metal oxides are present. The catalytic activity decreases when the metal oxides are extracted with glacial acetic acid or 0.5M H<sub>2</sub>SO<sub>4</sub>, with a greater decrease in the activity of the 800°C heat-treated material.
- 2) Low-cost alternatives: A number of natural products have been examined for oxygen reduction activity. Hemin and hematin appear promising.

- 3) Optimization of the structure: Thinner layers improve the oxygen and electrolyte transport.

### Aluminum Anodes

Testing the statistical analysis of data obtained on various previously prepared alloys and of some Alcan proprietary alloys has continued at Eltech. A research program was initiated at SRI International.

The tests at Eltech have been performed at 60°C in 4M NaOH; they measure the Open Circuit Corrosion Rate (OCC),  $\text{mg/cm}^2/\text{min}$ , which is almost equivalent to a corrosion current in  $\text{mA/cm}^2$ ; and, the Open Circuit Potential (OCP), -V vs Hg/HgO. In some tests they have incorporated .06M sodium stannate as corrosion inhibitor; in others, 1M of dissolved alloy. Polarization testing has been performed on the most promising alloys. Statistical analysis of data on alloys containing In, Tl, and Ga indicates that Ga does not significantly influence the OCC. Ga does have a strong effect in the OCP and cross terms are significant. The models predict improved voltage only at the expense of increased corrosion rate. One of the best alloys ESC-3, in the presence of 1M dissolved alloy, has an OCC of 0.029 (Zn yields .011) at an OCP of 1.78. The voltage decreases to 1.31 V at 600  $\text{mA/cm}^2$ .

Two Alcan proprietary alloys show promise with OCC of 0.12 and OCP of 1.84; one of these alloys gave 1.5 V at 500  $\text{mA/cm}^2$  in 4M NaOH at 60°C.

The work at SRI is aimed at developing a fundamental understanding of the processes taking place at the anode surface. They have calculated thermodynamic activities of the important species, and will interpret the results of complex impedance measurements in terms of the thermodynamics and kinetics of the various possible reactions. Experimentally, they have recently completed a cell with a well-defined hydrodynamic flow pattern to measure simultaneously the partial anodic and cathodic reactions occurring at the surface.

### Carbon Dioxide Scrubber

The detailed design has been ignored thus far because the amounts of carbon dioxide involved are small, less than 6 kg/yr. However, since the atmospheric  $\text{CO}_2$  concentration is about 330 ppm and the current specification calls for 2-5 ppm, about 99% removal of atmospheric  $\text{CO}_2$  is required at air

flow rates as high as 10 L/s. A preliminary calculation was made of the size of a packed tower absorber. The results of the calculations indicate that a packed tower absorber for vehicle application is at least 9 in. diameter by 68 in. high. While it is realized that packed columns are not appropriate, the above analysis does indicate that careful design is required.

It is likely that KOH will become the main component of the electrolyte rather than NaOH, because potassium carbonate is much more soluble than sodium carbonate. There are many other advantages to the use of KOH.

#### M4 Cell

Previous work demonstrated good performance and smooth feeding of the aluminum anode in the M3 cell.<sup>3</sup> In CY1984 the initial test of the M4 cell was performed, Fig. 5. The performance of the M4 cell in the M4-1 experiment was satisfactory, although the experiment objectives did not include testing of cell characteristics.

#### Electrolyte Flow

In the M4 cell electrolyte feeds from both sides into a flow distribution plenum; however, only one feed port was used in the M4-1 experiment. Upon disassembly we found that metallic tin and hydrargillite had deposited in the flow distribution plenum, starting about 3 in. from the inlet. A substantial amount of solids had also accumulated at the bottom of the wedge and in the anode/cathode gap. The deposit was heaviest opposite to the electrolyte inlet.

The M4 cell overflow feeds the internal return manifold through a series of openings in the back of each cell pod. Upon disassembly we found caked deposits of hydrargillite on the internal-cell-electrolyte-return manifold of one of the cell pods. The loosely adhering deposits, about 0.5 mm thick, were not likely to have been the source of plugging in the return line.

Subsequent experiments at Eltech with M4 cell pods have shown that the electrolyte flow past the anode/cathode space is not uniform. It is low at both ends of the electrode chamber; however, this was easily remedied by inserting a flow distributor into the inlet distribution plenum. The lack of uniformity in electrolyte flow reflected on the consumption of the aluminum anode; at the end of the run, it was about 7 mm longer near the edges than in the center.

In contrast to previous cells, the M4 cell is very easy to assemble and disassemble, thus it was possible to readily examine the result of system malfunctions without damaging the cell.

#### Air Flow

The M4 cell has air flow across the cell. There is concern that the unequal oxygen concentration on the two sides of a cell pod might lead to uneven consumption of the anode. At least for relatively short (4 h at 120 A) periods, anode consumption is relatively insensitive to oxygen concentration.

#### Air Cathode Assembly

Platinum catalyzed cathodes were used in the assembly of the M4-1 cell. The edges of the cathodes were glued to the pods using epoxy. A good bond was obtained with no pinhole air leaks, and with seams intact after the M4-1 experiment.

Good electrical connection to the metallic screen of the cathodes was more difficult to obtain. Two methods were used: soldering and conductive epoxies. Soldering was accomplished using low melting (93°C) indium solder; it gave a very good joint. Using conductive epoxy two pods were assembled; the bond failed in the first pod during assembly. A tougher epoxy was used for the second assembly. It appeared to be satisfactory after oven cure, but the current and voltage records of the M4-1 experiment indicate that the conductive epoxy bond failed during the run.

#### Cell Design at Eltech

Six M4 cell pods were given to Eltech for their cell development work. They found the electrolyte flow to be uneven, but also found an easy solution to the problem. The main emphasis of Eltech's work is in developing techniques for inexpensive assembly of air cathodes into the cell. They are studying a number of configurations in which the air cathode is assembled on a conductive frame and then the assembly is mounted onto the cell pod. Several methods of attaching the air cathode to its conductive frame are being evaluated.

## CRYSTALLIZATION

### Experimental

Experimental studies on crystallization and separation of hydrargillite from the electrolyte were carried out at LLNL and at Alcan. The LLNL M3-3 and M4-1 experimental results have already been described; this section will highlight the crystallization experiments at Alcan.<sup>10</sup>

### Alcan Crystallization Experiments

Alcan has carried out a large number of crystallization experiments at 60-80°C in 4M NaOH as well as a few experiments using KOH and KOH-NaOH mixtures. A schematic diagram of their equipment is shown in Fig. 6. The supersaturated aluminate solution (about 2.9M) added at a constant rate to the crystallization tank.

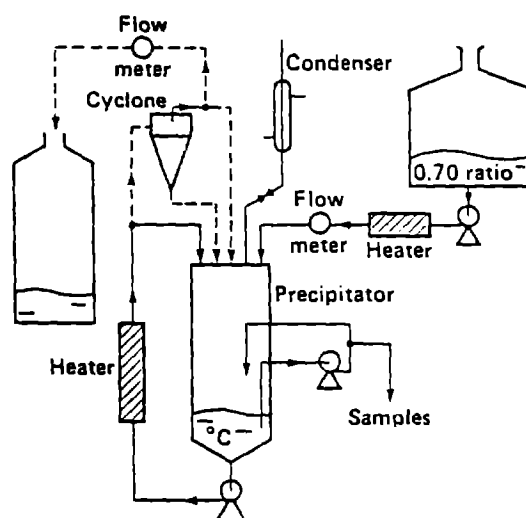


Fig. 6. Schematic of Alcan's crystallization equipment.

### Crystallization Kinetics

Alcan obtained a very good correlation for their experimental crystal growth rates (correlation coefficient 0.9985). In the NaOH system, the fastest growth rate occurs at 2.6M aluminate at 80°C; 3.1  $\mu\text{m/h}$ . It is about 15% lower at both 70° and 90°C. Precipitation from KOH yields approximately

the same rate, provided the seed was grown from KOH solution, but is lower with seed from NaOH solution.

### Agglomeration Experiments

Very significant results have been obtained at Alcan regarding agglomeration of hydrargillite. Under "high turbulence" conditions agglomeration does not proceed beyond the 10-20  $\mu\text{m}$  size; under "low turbulence" conditions the particles continue to agglomerate. The optimum agglomeration temperature, for both NaOH and KOH, appears to be about 80 °C. Figure 7 shows the evolution of the particle size distribution during a 2-h run at 84°C under low turbulence conditions; almost no secondary nucleation occurs at this temperature. The < 10  $\mu\text{m}$  fraction of the population is negligible after 50 min; the 10-20  $\mu\text{m}$  population peaks at about 50 min and is negligible after 105 min; the 20-30  $\mu\text{m}$  population begins to increase rapidly at 90 min and is peaking at 145 min; the greater than 40  $\mu\text{m}$  population begins to grow at about 110 min and constitutes about 25% of the total product weight after 2 h. Thus, agglomeration can provide the desired product particle size in reasonably short times.

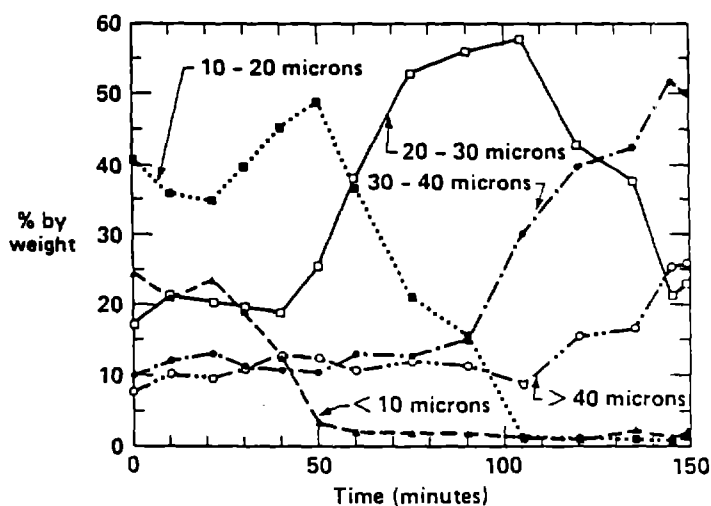


Fig. 7. Agglomeration and particle growth during crystallization experiment at Alcan.

## Crystallization Modeling

A computer code CRYSP, written at LLNL, predicts how the particle size distribution evolves as a function of vehicle operating conditions. CRYSP was written as a main driver code, which handles the input output and describes the system configuration by the interconnections between the various components, and a collection of subroutines which describe in detail the behaviour of the various components. In its present configuration it has subroutines which describe: 1) cell performance parameters (power, heat balances, material balances, water evaporation and make-up, etc.), 2) a mixed suspension and mixed product removal (MSMPR) crystallizer, 3) hydrocyclone, 4) mixing blocks, 5) particle growth using Alcoa's correlation, and 6) an arbitrary secondary nucleation source.

A good fit to the M3-3 results (particle size distributions vs time) was obtained when the nucleation source was set to match the experimental value of the M3-3 run.

As additional experimental data and correlations are obtained, the particle description in CRYSP will be modified with subroutines to describe secondary nucleation, particle attrition and agglomeration. No effort is being devoted at present to further code development.

## INSTRUMENTATION DEVELOPMENT

### Correlations of aluminate conductivity

The data of Landrum<sup>7</sup>, Alcoa<sup>8</sup> and Alcan<sup>9</sup> were examined in detail. While each set is internally consistent, there are large systematic differences between the data sets; the data recently obtained at LLNL has not been analyzed in detail.

### Particle size measurements

Particle size measurements are a critical part of analysis of crystallization behavior. Intercomparison of analyses on the same samples at Alcan and LLNL has shown very good agreement.

## REFERENCES

1. I. B. Weinstock, DOE Battery Development Program Hardware Performance Status-1984, Aerospace Corp., Washington, D.C., ATR-84(4821-04)-1ND (1984).
2. L.G. O'Connell, et al., Energy Storage Systems for Automobile Propulsion: Final Report, Vol. 2: Energy Storage Devices, Lawrence Livermore National Laboratory, Livermore, CA, UCRL-53053 Vol. 2, (1980), pp. 1-1 through 1-26.
3. J. F. Cooper, Aluminum-Air Power Cell Research and Development Progress Report, presented at the Electric and Hybrid Vehicle Systems Assessment Seminar, Gainesville, FL, Dec. 15-16, 1983; published as Lawrence Livermore National Laboratory, Livermore, CA, UCRL-90465, (1984).
4. A. Maimoni and S.A. Muelder, Aluminum-Air Power Cell: The M3-3 Experiment, to be published as Lawrence Livermore National Laboratory Report UCID-20307, (1985).
5. M. Newman, Development of Hydrocyclones for Aluminum-Air Battery Applications, Lawrence Livermore National Laboratory, Livermore, CA, UCID-20061, (1984).
6. L.A. Knerr and D.J. Wheeler, "Aluminum/Air Battery Development, Final Report Under Contract No. 5033001," Eltech Systems Corp, Fairport Harbor, OH. Limited distribution report of February 15, 1985.
7. J.H. Landrum, Electrical Conductivity of Caustic Aluminate Solutions at Various Concentrations and Temperatures, Lawrence Livermore National Laboratory, Livermore, CA, UCID-18339, (1980).
8. T.G. Swansiger, C. Misra, and F.S. Williams, Development and Demonstration of Process and Components for the Control of Aluminum-Air Battery Composition through the Precipitation of Aluminum Hydroxide, Aluminum Company of America, Final Report under subcontract 5724709; Lawrence Livermore National Laboratory, Livermore, CA, UCRL-15503, (1982).
10. B. O'Callaghan, Alcan Kingston Laboratories, Kingston, Ontario, private communication, 1984.